



HAL
open science

Fractional modeling of gradual incorporation of infected prey into the predator-prey system with consideration of seasonality

Seda Icret Araz, Salah Boulaaras

► To cite this version:

Seda Icret Araz, Salah Boulaaras. Fractional modeling of gradual incorporation of infected prey into the predator-prey system with consideration of seasonality. 2025. <hal-04929853>

HAL Id: hal-04929853

<https://hal.science/hal-04929853v1>

Preprint submitted on 5 Feb 2025

HAL is a multi-disciplinary open access archive for the deposit and dissemination of scientific research documents, whether they are published or not. The documents may come from teaching and research institutions in France or abroad, or from public or private research centers.

L'archive ouverte pluridisciplinaire **HAL**, est destinée au dépôt et à la diffusion de documents scientifiques de niveau recherche, publiés ou non, émanant des établissements d'enseignement et de recherche français ou étrangers, des laboratoires publics ou privés.



HAL Authorization

Fractional modeling of gradual incorporation of infected prey into the predator-prey system with consideration of seasonality

Seda Icret Araz¹ and Salah Boulaaras²

¹Department of Mathematics Education, Faculty of Education, Siirt University, Turkey.

²Department of Mathematics, College of Science, Qassim University, Saudi Arabia.

January 30, 2025

Abstract

Prey-predator models are essential for understanding the dynamics of ecological systems, where predators consume prey and population fluctuations are influenced by factors such as birth rates, death rates, and resource availability. The Lotka-Volterra model is a classical example, where prey populations grow exponentially in the absence of predators, and predator populations increase with the availability of prey. However, real-world ecosystems become more complex, particularly when diseases affect prey populations. Infected prey may exhibit altered behaviors or reduced fitness, making them more vulnerable to predation, thereby impacting both prey and predator populations. To model these interactions more realistically, disease dynamics will be incorporated to investigate the effects of infections on species behavior, survival, and ecosystem stability. The gradual introduction of infected prey into the population will be modeled using an advanced framework of partial differential equations, which includes fractional derivatives to capture memory effects and non-local interactions. Furthermore, the model will incorporate almost periodic functions to account for seasonality, effectively reflecting the cyclical nature of environmental fluctuations.

Keywords: Ecological models, seasonality, piecewise modeling, fractional differentiation and integration, almost periodicity.

1 Introduction

Prey-predator models are fundamental in understanding the dynamics of ecological systems, where two species interact in a way that one (the predator) hunts and consumes the other (the prey) [1-5]. These models, often described using mathematical equations, help explain how the populations of both species fluctuate over time, driven by factors such as birth rates, death rates, and the availability of resources. The classic Lotka-Volterra model is one of the most well-known frameworks used to represent these interactions, where the prey population grows exponentially in the absence of predators, and the predator population grows in response to increased availability of prey. However, real-world ecological systems are often more complex than these simple models suggest. One important complexity arises when disease enters the equation, particularly when the prey species becomes infected. The introduction of infected prey changes the dynamics of the predator-prey interaction, as the infected individuals may exhibit altered behavior or reduced fitness, which can make them more vulnerable to predation or less capable of evading predators. This shift in prey behavior and population health introduces additional layers of complexity, as the disease can affect not only the prey species but also the predators, creating a feedback loop that influences both populations. Incorporating

disease dynamics into prey-predator models offers a more realistic representation of ecological interactions, as it highlights the role of infection in shaping species behavior, survival, and population fluctuations. These models allow researchers to explore how pathogens influence ecological outcomes, such as predator-prey ratios, disease transmission between species, and the overall stability of ecosystems. The study of infected prey populations in such models is critical for understanding the broader impacts of disease on biodiversity and the resilience of natural communities [6-11].

Let us provide a motivation for understanding and interpreting such a process. In an ecological context, consider a forest ecosystem where rabbits (prey) serve as the primary food source for wolves (predators). Within this system, a viral infection begins to spread through a portion of the rabbit population. Infected rabbits exhibit behavioral changes such as reduced alertness and slower movements, which make them more susceptible to predation. However, the wolves, in consuming these infected rabbits, risk contracting the virus themselves. As the disease continues to proliferate, the rabbit population begins to decline, leading to a reduction in the prey availability for the wolves. Consequently, the wolf population faces a decrease in food resources, which ultimately leads to a decline in predator numbers due to the scarcity of prey. At the same time, although the infected rabbits continue to reproduce, their weakened state results in lower survival rates, further exacerbating the decline in the prey population. This results in a complex feedback loop where the interactions between the infected prey and the predators significantly alter both populations. The system reaches a fragile equilibrium, where the disease modifies predator-prey dynamics by simultaneously influencing the health, behavior, and population sizes of both species. Such interactions emphasize the profound impact that disease can have on the structure of ecological communities. Infected prey not only affect their own survival but also shape the strategies and survival of predators, thus illustrating the intricate interplay of biological, behavioral, and environmental factors in shaping ecosystem dynamics.

To further enrich the model, seasonality can be incorporated as a key factor influencing the dynamics of both prey and predator populations [12]. Seasonal changes, such as variations in temperature, food availability, and reproductive cycles, can significantly affect the birth and death rates of both species. For example, in temperate ecosystems, the availability of prey may fluctuate seasonally due to changes in vegetation growth, which in turn impacts predator food supply. Similarly, predators may exhibit seasonal variations in hunting efficiency, reproduction, and mortality, influenced by environmental conditions such as temperature and daylight hours. Seasonality can also interact with disease dynamics, as certain pathogens may have seasonal transmission patterns, with higher infection rates during specific months or periods of the year. Infected prey may, therefore, experience different survival rates across seasons, affecting the overall population dynamics of both prey and predators. By introducing seasonality into prey-predator models, a more realistic and comprehensive understanding of ecological interactions can be achieved, capturing the complexities of how environmental factors and disease dynamics together shape the structure and stability of ecosystems over time.

Therefore, in this study, to enhance the realism of the model, we considered a population initially free of infected prey, with infected individuals being introduced after a certain period. Additionally, the effects of seasonality under varying environmental conditions were incorporated to more accurately reflect the dynamic interactions within the ecosystem. The introduction of infected prey into the population over time will be modeled through the piecewise setting [13], while seasonality will be incorporated using almost periodic functions to capture the cyclical nature of environmental conditions [12]. Additionally, the inclusion of infected prey into the population over time will be modeled using piecewise differential equations, incorporating fractional derivatives to account for memory effects and non-local interactions in the system.

Let ${}^C D_t^\kappa \chi(t)$ be the Caputo fractional derivative [15], ${}^{CF} D_t^\kappa \chi(t)$ be the fractional derivative with the exponential decay kernel (CF) [16], ${}^{AB} D_t^\kappa \chi(t)$ be the fractional derivative with the Mittag-Leffler kernel (AB) [17] and ${}^{RL} D_t^\kappa \chi(t)$ be the Riemann-Liouville fractional derivative [18]. If χ be a function continuously differentiable, these derivatives in Caputo sense are defined as

$${}^C D_t^\kappa \chi(t) = \frac{1}{\Gamma(1-\kappa)} \int_{t_0}^t \chi'(\varsigma) (t-\varsigma)^{-\kappa} d\varsigma, \quad (1)$$

$${}^{CF} D_t^\kappa \chi(t) = \frac{1}{1-\kappa} \int_{t_0}^t \chi'(\varsigma) \exp\left(-\frac{\kappa}{1-\kappa}(t-\varsigma)\right) d\varsigma, \quad (2)$$

$${}^{ABC} D_t^\kappa \chi(t) = \frac{1}{1-\kappa} \int_{t_0}^t \chi'(\varsigma) E_\kappa\left(-\frac{\kappa}{1-\kappa}(t-\varsigma)^\kappa\right) d\varsigma. \quad (3)$$

If χ is continuous, these derivatives in Riemann-Liouville sense are defined as

$${}^{RL} D_t^\kappa \chi(t) = \frac{1}{\Gamma(1-\kappa)} \frac{d}{dt} \int_{t_0}^t \chi(\varsigma) (t-\varsigma)^{-\kappa} d\varsigma, \quad (4)$$

$${}^{CF} D_t^\kappa \chi(t) = \frac{1}{1-\kappa} \frac{d}{dt} \int_{t_0}^t \chi(\varsigma) \exp\left(-\frac{\kappa}{1-\kappa}(t-\varsigma)\right) d\varsigma, \quad (5)$$

$${}^{ABC} D_t^\kappa \chi(t) = \frac{1}{1-\kappa} \frac{d}{dt} \int_{t_0}^t \chi(\varsigma) E_\kappa\left(-\frac{\kappa}{1-\kappa}(t-\varsigma)^\kappa\right) d\varsigma, \quad (6)$$

where $0 < \kappa < 1$. Here, Mittag-Leffler and exponential function are defined as

$$E_\kappa(-\zeta t^\kappa) = \sum_{m=0}^{\infty} \frac{(-\zeta t^\kappa)^m}{\Gamma(\kappa m + 1)}, \quad (7)$$

and

$$\exp(-\zeta t) = \sum_{m=0}^{\infty} \frac{(-\zeta t)^m}{m!}. \quad (8)$$

2 Prey-infected prey-predator system

In this section, various analyses will be presented concerning the model [11], which addresses prey-predator interactions within a population that includes both predators and infected prey. The model under investigation [11] is represented by the following system

$$\begin{cases} \frac{dP_1}{dt} = a(P_1 + I) - bP_1 - cP_1(P_1 + I) - kIP_1 - \mu P_1 P_2, \\ \frac{dI}{dt} = kIP_1 - bI - cP_1(P_1 + I) - \gamma IP_2, \\ \frac{dP_2}{dt} = \theta P_1 P_2 - \sigma IP_2 - \rho P_2 \end{cases}, \quad (9)$$

where $c = \frac{a-b}{M}$, $a > b$. The functions $P_1(t)$, $P_2(t)$ and $I(t)$ represent, respectively, the susceptible prey, the infected prey, and the predator at time t . These functions serve as key components in modeling the

dynamics of the prey-predator-infection system. A detailed description of the parameters used in this model is provided in Table 1.

Table 1. The explanations of the model parameters

Parameter	Explanation
a	The birth rate
b	The intrinsic death rate
M	The environmental carrying capacity
k	The infection coefficient
μ	The predator's rate of attacking the vulnerable prey
γ	The predator's rate of attacking the infected prey
θ	Conversion rate of the susceptible
σ	Conversion rate of the infected.
ρ	The intrinsic death rate of predator
c	The depletion of the food supply

Disease-free equilibrium point of this system is

$$\left(\frac{\rho}{\theta}, 0, \frac{a\theta - b\theta - c\rho}{\theta\mu} \right), \quad (10)$$

where $a > b + \frac{c\rho}{\theta}$ and endemic equilibrium point of this system is

$$\left(\frac{a}{k}, \frac{k\rho - a\theta}{k\theta}, \frac{a\theta - b\theta - c\rho}{\theta\mu} \right). \quad (11)$$

where $b + \frac{c\rho}{\theta} < a < \frac{k\rho}{\theta}$. To obtain the reproduction number, we need to check the transition matrices

$$\begin{aligned} \partial F &= [kP_1 - cP_1 - \gamma P_2], \\ \partial V^{-1} &= \begin{bmatrix} 1 \\ b \end{bmatrix} \end{aligned} \quad (12)$$

The spectral radius of the (FV^{-1}) , also known as the reproduction number, is calculated as:

$$R_0 = \frac{(k - c)\rho\mu - \gamma(a\theta - b\theta - c\rho)}{b\theta\mu}. \quad (13)$$

where $(k - c)\rho\mu > \gamma(a\theta - b\theta - c\rho)$.

3 A piecewise differential equation modeling the gradual incorporation of infected prey into an ecological system

In this section, the model addressing prey-predator interactions within a population, where both prey-predator dynamics and infected prey are considered, will be modified employing the concept of piecewise differential equations to capture reality. Initially, the model will describe the interaction between prey and predators in the population, followed by the gradual introduction of infected prey over time. The model in question is governed by the following equations:

$$\left\{ \begin{array}{l} \frac{dP_1}{dt} = aP_1 - bP_1 - \mu P_1 P_2, \\ \frac{dP_2}{dt} = \theta P_1 P_2 - \rho P_2 \end{array} \right., \text{ if } 0 \leq t \leq t_1, \quad (14)$$

$$\left\{ \begin{array}{l} \frac{dP_1}{dt} = a(P_1 + I) - bP_1 - cP_1(P_1 + I) - kIP_1 - \mu P_1 P_2, \\ \frac{dI}{dt} = kIP_1 - bI - cP_1(P_1 + I) - \gamma IP_2, \\ \frac{dP_2}{dt} = \theta P_1 P_2 - \sigma IP_2 - \rho P_2 \end{array} \right., \text{ if } t_1 \leq t \leq \hat{T},$$

It is crucial to highlight that the model presented in [11] is reformulated as a piecewise differential equation, where the infected prey is absent (i.e. $I(t) = 0$) from the population during the interval $0 \leq t \leq t_1$, and infected prey is incorporated into the system in the interval $t_1 \leq t \leq \hat{T}$. In Figure 1, we visualize the scenario mentioned here to understand the process.

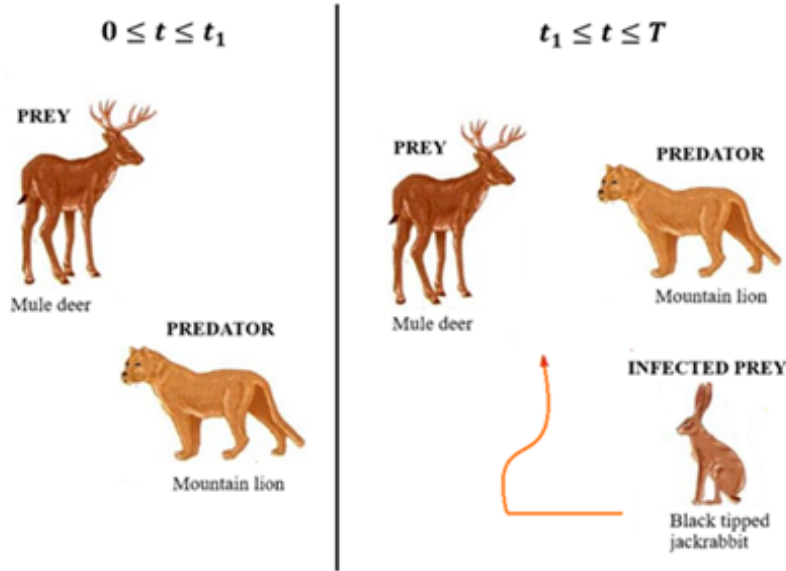
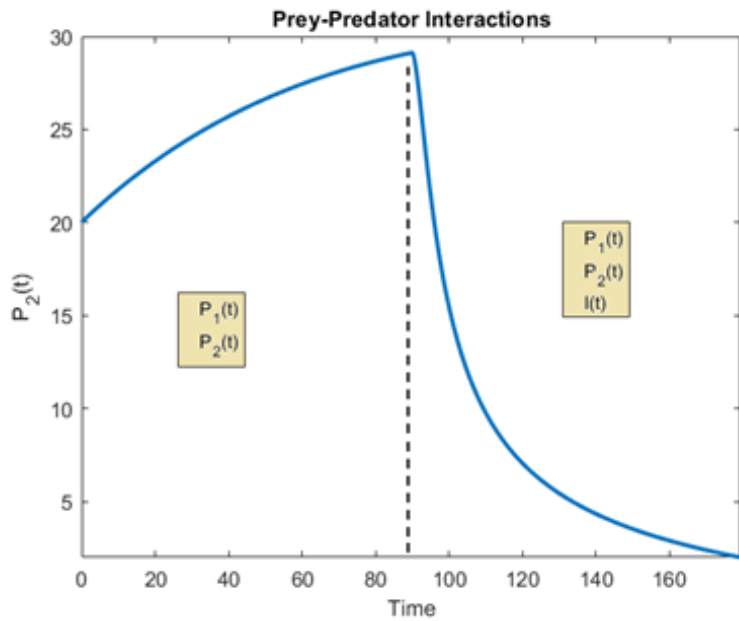
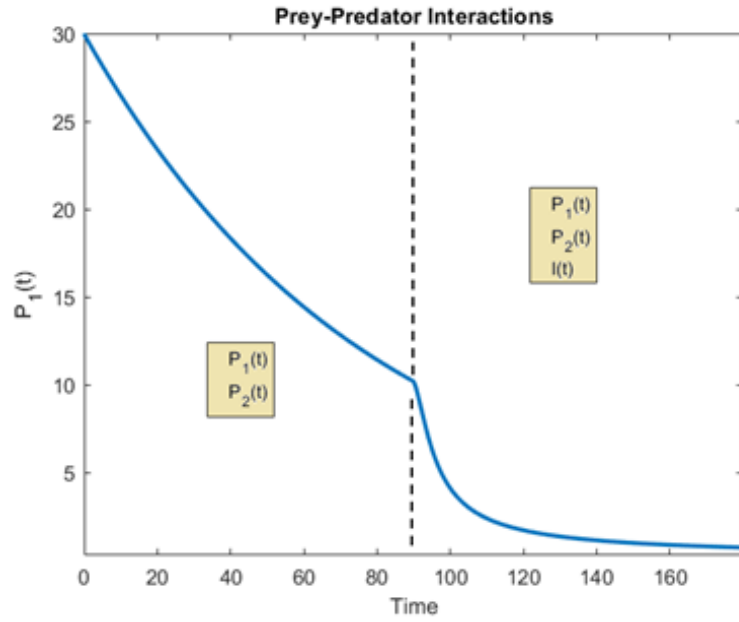


Figure 1. The visualization of the scenario depicting the gradual incorporation of infected prey into a prey-predator system.

Figure 1 illustrates a simulation period in which only the mule deer and mountain lion are present in the population within the interval $0 \leq t \leq t_1$, while the infected black-tipped jackrabbit is introduced into the population within the interval $t_1 \leq t \leq \hat{T}$. It is clear that such a scenario is not only possible in nature but also more realistic compared to a scenario in which prey, infected prey, and predators coexist within a single time period. Such a scenario will be simulated by considering the following initial conditions and parameters:

$$\begin{aligned} P_1(0) &= 30; I(0) = 0; P_2(0) = 20; a = 0.001; k = 0.001; \theta = 0.15; \\ \rho &= 0.7; \mu = 0.265; b = 0.0001; c = 0.0035; \sigma = 0.25; \gamma = 0.02. \end{aligned}$$

Figure 2 presents the graphical simulation of the piecewise differential equation that models the integration of infected prey into an ecological system.



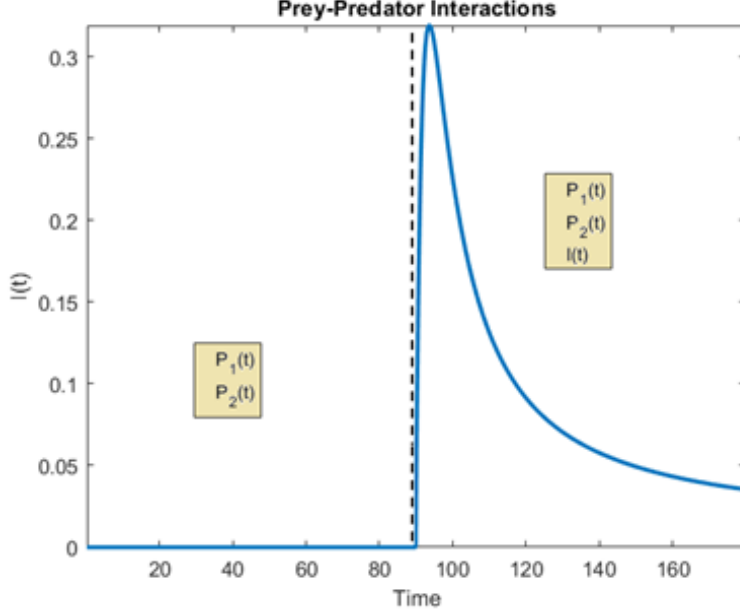


Figure 2. The visualization of the scenario depicting the gradual incorporation of infected prey into prey-predator system.

3.1 Existence and uniqueness of solutions for the piecewise ecological system

The analysis of the existence and uniqueness of solutions employing mathematical methods is essential for addressing real-world challenges. Although this theory has been effectively applied to both integer and noninteger-order differential equations, there is relatively little research dedicated to its application to this new class of differential equations [13] with piecewise derivatives [21]. In this section, we specify the conditions under which the solutions of piecewise model are both unique and exist [3, 19]. To simplify the presentation, we first introduce the following notations:

$$\begin{aligned} \Pi = \eta_m &= \begin{bmatrix} P_1 \\ P_2 \end{bmatrix}, F(\Pi, t) = \chi_m(t, \eta_m) = \begin{bmatrix} aP_1 - bP_1 - \mu P_1 P_2 \\ \theta P_1 P_2 - \rho P_2 \end{bmatrix}, \\ \Sigma = \eta_n &= \begin{bmatrix} P_1 \\ P_2 \\ P_3 \end{bmatrix}, G(\Sigma, t) = \chi_n(t, \eta_n) = \begin{bmatrix} a(P_1 + I) - bP_1 - cP_1(P_1 + I) - kIP_1 - \mu P_1 P_2 \\ kIP_1 - bI - cP_1(P_1 + I) - \gamma IP_2 \\ \theta P_1 P_2 - \sigma IP_2 - \rho P_2 \end{bmatrix}. \end{aligned} \quad (15)$$

Lemma 1. Using the definition in [13], the solution of the following piecewise differential equation

$$\begin{cases} \frac{d\Pi}{dt} = F(\Pi, t), & \text{if } 0 \leq t \leq t_0. \\ {}_{t_0}^{ABC} D_t^\kappa \Sigma(t) = G(\Sigma, t), & \text{if } t_0 \leq t \leq \hat{T}. \end{cases} \quad (16)$$

is represented by

$$X(t) = \begin{cases} \left\{ \begin{array}{l} \eta_m(0) + \int_0^t \chi_m(\vartheta, \eta_m(\vartheta)) d\vartheta, m = 1, 2, \text{ if } 0 \leq t \leq t_0, \\ \eta_n(t_0) + (1 - \kappa) \chi_n(\vartheta, \eta_n(\vartheta)) \\ + \frac{\kappa}{\Gamma(\kappa)} \int_{t_0}^t \chi_n(\vartheta, \eta_n(\vartheta)) (t - \vartheta)^{\kappa-1} d\vartheta, n = 1..3, \text{ if } t_0 \leq t \leq \widehat{T}, \end{array} \right. \end{cases} \quad (17)$$

where $0 < \kappa < 1$, $\chi : [0, \widehat{T}] \times \mathbb{R} \rightarrow \mathbb{R}$.

Let us define the following mapping $\Lambda : \Omega \rightarrow \Omega$ (Ω , Banach space) given by

$$\Lambda\Pi(t) = \begin{cases} \left\{ \begin{array}{l} \eta_m(0) + \int_0^t \chi_m(\vartheta, \eta_m(\vartheta)) d\vartheta, m = 1, 2, \text{ if } 0 \leq t \leq t_0, \\ \eta_n(t_0) + (1 - \kappa) \chi_n(\vartheta, \eta_n(\vartheta)) \\ + \frac{\kappa}{\Gamma(\kappa)} \int_{t_0}^t \chi_n(\vartheta, \eta_n(\vartheta)) (t - \vartheta)^{\kappa-1} d\vartheta, n = 1..3, \text{ if } t_0 \leq t \leq \widehat{T} \end{array} \right. \end{cases} \quad (18)$$

To prove this, we assume that the following conditions hold true [14]:

K1) For all $\eta_1, \eta_2 \in \mathbb{R}$, two constants ν_1, ν_2 exist so that the following inequalities hold

$$\begin{aligned} |\chi_m(t, \eta) - \chi_m(t, \delta)| &\leq \nu_1 |\eta - \delta|, \\ |\chi_n(t, \eta) - \chi_n(t, \delta)| &\leq \nu_2 |\eta - \delta|. \end{aligned} \quad (19)$$

K2) There exist functions $\widetilde{\nu}_1(\vartheta), \widetilde{\nu}_2(\vartheta)$ such that

$$\begin{aligned} |\chi_m(t, \eta) - \chi_m(t, \delta)| &\leq \widetilde{\nu}_1(\vartheta) |\eta| + \widetilde{L}_1(\vartheta), \\ |\chi_n(t, \eta) - \chi_n(t, \delta)| &\leq \widetilde{\nu}_2(\vartheta) |\eta| + \widetilde{L}_2(\vartheta). \end{aligned} \quad (20)$$

Theorem 1. Given hypothesis **K1)**, the considered equation possesses one solution provided that the statement presented below is satisfied.[14]:

$$\nu = \max \left\{ \nu_1 t_0, \nu_2 \left[(1 - \kappa) + \frac{(\widehat{T} - t_0)^\kappa}{\Gamma(\kappa)} \right] \right\} < 1. \quad (21)$$

Proof. It is necessary to prove that Λ is indeed a contraction. To demonstrate this, we proceed by expressing

$$\|\Lambda\eta - \Lambda\delta\| \leq \sup_{t \in [0, \widehat{T}]} \left\{ \left\{ \begin{array}{l} \int_0^t |\chi_m(\vartheta, \eta(\vartheta)) - \chi_m(\vartheta, \delta(\vartheta))| d\vartheta, \text{ if } 0 \leq t \leq t_0, \\ (1 - \kappa) |\chi_n(t, \eta(t)) - \chi_n(t, \delta(t))| \\ + \frac{\kappa}{\Gamma(\kappa)} \int_{t_0}^t |\chi_n(\vartheta, \eta(\vartheta)) - \chi_n(\vartheta, \delta(\vartheta))| (t - \vartheta)^{\kappa-1} d\vartheta \text{ if } t_0 \leq t \leq \widehat{T} \end{array} \right. \right\}. \quad (22)$$

Using the hypothesis **K1)**, we have

$$\|\Lambda\eta - \Lambda\delta\| \leq \sup_{t \in [0, \widehat{T}]} \left\{ \left[\begin{array}{l} \nu_1 |\eta - \delta| t_0, \text{ if } 0 \leq t \leq t_0, \\ \left[(1 - \kappa) + \frac{(\widehat{T} - t_0)^\kappa}{\Gamma(\kappa)} \right] \nu_2 |\eta - \delta|, \text{ if } t_0 \leq t \leq \widehat{T}. \end{array} \right] \right\}. \quad (23)$$

Therefore, we obtain

$$\|\Lambda\eta - \Lambda\delta\| \leq \nu \|\eta - \delta\|, \quad (24)$$

where

$$\nu = \max \left\{ \nu_1 t_0, \nu_2 \left[(1 - \kappa) + \frac{(\widehat{T} - t_0)^\kappa}{\Gamma(\kappa)} \right] \right\}. \quad (25)$$

Since $\nu < 1$, we can conclude that the mapping Λ is contraction.

Theorem 2. The piecewise differential equation presented here has at least one solution under the conditions **K1**, **K2**.

Proof. Initially, a mapping is constructed to perform our aim

$$\bar{\Lambda}\eta = \begin{cases} \left\{ \begin{array}{l} \eta_m(0) + \int_0^{t_0} \chi_m(\vartheta, \eta(\vartheta)) d\vartheta, m = 1, 2, \text{ if } 0 \leq t \leq t_0, \\ \eta_n(t_0) + (1 - \kappa) |\chi_n(t, \eta(t)) - \chi_n(t, \delta(t))| \\ + \frac{\kappa}{\Gamma(\kappa)} \int_{t_0}^t \chi_n(\vartheta, \eta(\vartheta)) (t - \vartheta)^{\kappa-1} d\vartheta, n = 1..3, \text{ if } t_0 \leq t \leq \widehat{T} \end{array} \right. \end{cases} \quad (26)$$

By employing **K2**, we need to demonstrate that Λ is completely continuous. Applying norm on both sides, we achieve

$$\|\bar{\Lambda}\eta\| \leq \sup_{t \in [0, \widehat{T}]} \begin{cases} \left\{ \begin{array}{l} \int_0^{t_0} (|\nu_1(\vartheta)| \|\eta\| + L_1(\vartheta)) d\vartheta, \text{ if } 0 \leq t \leq t_0, \\ (1 - \kappa) |\chi_n(t, \eta(t)) - \chi_n(t, \delta(t))| \\ + \frac{\kappa}{\Gamma(\kappa)} \int_{t_0}^t (|\nu_2(\vartheta)| \|\eta\| + L_2(\vartheta)) d\vartheta, \text{ if } t_0 \leq t \leq \widehat{T}, \end{array} \right. \end{cases} \quad (27)$$

which yields

$$\|\bar{\Lambda}\eta\| \leq \sup_{t \in [0, \widehat{T}]} \begin{cases} \left\{ \begin{array}{l} t_0 (\tilde{\nu}_1 \epsilon + \tilde{L}_1), \text{ if } 0 \leq t \leq t_0, \\ (\tilde{\nu}_2 \epsilon + \tilde{L}_2) \left(1 - \kappa + \frac{(\widehat{T} - t_0)^\kappa}{\Gamma(\kappa)} \right), \text{ if } t_0 \leq t \leq \widehat{T}, \end{array} \right. \end{cases} \quad (28)$$

where $\epsilon = \|\eta\| = \sup_{t \in [0, \widehat{T}]} |\eta|$, $\widehat{\nu}_1 = \sup_{t \in [0, \widehat{T}]} |\tilde{\nu}_1(\vartheta)|$, $\widehat{\nu}_2 = \sup_{t \in [0, \widehat{T}]} |\tilde{\nu}_2(\vartheta)|$, $\widehat{L}_1 = \sup_{t \in [0, \widehat{T}]} |\tilde{L}_1(\vartheta)|$, $\widehat{L}_2 = \sup_{t \in [0, \widehat{T}]} |\tilde{L}_2(\vartheta)|$.

Here, we choose $\tilde{\nu}$ such that

$$\tilde{\nu} = \max \left\{ t_0 (\widehat{\nu}_1 \epsilon + \widehat{L}_1), (\widehat{\nu}_2 \epsilon + \widehat{L}_2) \left(1 - \kappa + \frac{(\widehat{T} - t_0)^\kappa}{\Gamma(\kappa)} \right) \right\}. \quad (29)$$

Then, one can have the following

$$\|\bar{\Lambda}\eta\| \leq \tilde{\nu}. \quad (30)$$

This confirms that $\bar{\Lambda}$ is uniformly bounded, and next, we will demonstrate the equicontinuity of Λ . For $t_1 < t_2 \in [0, \widehat{T}]$, we obtain the following inequality:

$$\begin{aligned} |\Lambda\eta(t_2) - \Lambda\eta(t_1)| &= \left| \begin{cases} \int_0^{t_2} \chi_m(\vartheta, \eta(\vartheta)) d\vartheta - \int_0^{t_1} \chi_m(\vartheta, \eta(\vartheta)) d\vartheta, \text{ if } 0 \leq t \leq t_0, \\ \frac{1}{\Gamma(\kappa)} \int_{t_0}^{t_2} \chi_n(\vartheta, \eta(\vartheta)) (t_2 - \vartheta)^{\kappa-1} d\vartheta \\ - \frac{1}{\Gamma(\kappa)} \int_{t_0}^{t_1} \chi_n(\vartheta, \eta(\vartheta)) (t_1 - \vartheta)^{\kappa-1} d\vartheta \text{ if } t_0 \leq t \leq \widehat{T}. \end{cases} \right| \quad (31) \\ &\leq \left| \begin{array}{l} (\tilde{\nu}_1 \epsilon + \tilde{L}_1) |t_2 - t_1| \\ (1 - \kappa) (\tilde{\nu}_2 \epsilon + \tilde{L}_2) + \frac{\kappa}{\Gamma(\kappa)} (\tilde{\nu}_2 \epsilon + \tilde{L}_2) \left[- \int_{t_0}^{t_1} ((t_2 - \vartheta)^{\kappa-1} - (t_1 - \vartheta)^{\kappa-1}) d\vartheta \right] \end{array} \right|. \end{aligned}$$

Using the mean value theorem, we compute the integral of as follows:

$$\begin{aligned} \int_{t_1}^{t_2} (t_2 - \vartheta)^{\kappa-1} d\vartheta + \int_{t_0}^{t_1} \begin{pmatrix} (t_2 - \vartheta)^{\kappa-1} \\ -(t_1 - \vartheta)^{\kappa-1} \end{pmatrix} d\vartheta &= \frac{(t_2 - t_1)^\kappa}{\kappa} + (1 - \kappa) \begin{pmatrix} (t_1 - \epsilon)^{\kappa-2} \\ -(t_0 - \epsilon)^{\kappa-2} \end{pmatrix} (t_2 - t_1) \\ &= \tilde{\nu}(\epsilon, \kappa) \end{aligned} \quad (32)$$

Replacing this calculation into above inequality, we have

$$|\Lambda\eta(t_2) - \Lambda\eta(t_1)| \leq \begin{cases} (\tilde{\nu}_1\epsilon + \tilde{L}_1) |t_2 - t_1|, & \text{if } 0 \leq t \leq t_0, \\ (\tilde{\nu}_2\epsilon + \tilde{L}_2) \left(1 - \kappa + \frac{(\tilde{\nu}_2\epsilon + \tilde{L}_2)}{\Gamma(\kappa)} \tilde{\nu}(\epsilon, \kappa) \right) |t_2 - t_1|, & \text{if } t_0 \leq t \leq \hat{T}. \end{cases} \quad (33)$$

Then, we obtain the following:

$$|\Lambda\eta(t_2) - \Lambda\eta(t_1)| \leq \tilde{C}_1 |t_2 - t_1|, \quad (34)$$

where

$$\tilde{C} = \max \left\{ \tilde{\nu}_1\epsilon + \tilde{L}_1, (\tilde{\nu}_2\epsilon + \tilde{L}_2) \left(1 - \kappa + \frac{(\tilde{\nu}_2\epsilon + \tilde{L}_2)}{\Gamma(\kappa)} \tilde{\nu}(\epsilon, \kappa) \right) \right\}. \quad (35)$$

Thus, Λ is equicontinuous and compact. By applying the Arzelà-Ascoli theorem, we establish that the mapping Λ is uniformly continuous. Utilizing Krasnoselskii's fixed point theorem, it can be concluded that at least one solution exists for the equation presented here.

Theorem 3: To establish uniqueness, it is assumed that for all $\forall t \in [t_0, \hat{T}]$, a constant $\exists \nu > 0$ exists such that

$$\begin{aligned} |\chi_m(t, \eta) - \chi_m(t, \delta)| &\leq \tilde{c}_1 |\eta - \delta|, \\ |\chi_n(t, \eta) - \chi_n(t, \delta)| &\leq \tilde{c}_2 |\eta - \delta|. \end{aligned} \quad (36)$$

Under the condition presented above, the solution is shown to be unique.

Proof. It is assumed that the piecewise differential equation possesses two distinct solutions such that $\eta(t)$ and $\delta(t)$

$$|\eta(t) - \delta(t)| \leq \begin{cases} \int_0^t |\chi_m(\vartheta, \eta(\vartheta)) - \chi_m(\vartheta, \delta(\vartheta))| d\vartheta, & \text{if } 0 \leq t \leq t_0 \\ \begin{cases} (1 - \kappa) |\chi_n(t, \eta(t)) - \chi_n(t, \delta(t))| \\ + \frac{\kappa}{\Gamma(\kappa)} \int_{t_0}^t |\chi_n(\vartheta, \eta(\vartheta)) - \chi_n(\vartheta, \delta(\vartheta))| (t - \vartheta)^{\kappa-1} d\vartheta \end{cases} & \text{if } t_0 \leq t \leq \hat{T} \end{cases} \quad (37)$$

By the help of the Lipschitz condition, we obtain

$$|\eta(t) - \delta(t)| \leq \begin{cases} \tilde{c}_1 \int_0^t |\eta(\vartheta) - \delta(\vartheta)| d\vartheta, & \text{if } 0 \leq t \leq t_0 \\ \frac{(\hat{T} - t_0)^\kappa}{(1 - (\kappa - 1)) \Gamma(\kappa)} \tilde{c}_2 \int_{t_0}^t |\eta(\vartheta) - \delta(\vartheta)| d\vartheta & \text{if } t_0 \leq t \leq \hat{T}. \end{cases} \quad (38)$$

Using the Gronwall inequality, we have

$$|\eta(t) - \delta(t)| \leq \alpha \exp \begin{cases} \tilde{c}_1 |\eta - \delta| (t - t_0), & \text{if } 0 \leq t \leq t_0, \\ \tilde{c}_2 |\eta - \delta| \frac{(\hat{T} - t_0)^\kappa}{(1 - (\kappa - 1)) \Gamma(\kappa)}, & \text{if } t_0 \leq t \leq \hat{T}. \end{cases} \quad (39)$$

Here $\alpha = 0$ which leads to

$$\varphi(t) = 0 \Rightarrow \eta(t) = \delta(t). \quad (40)$$

This completes the proof.

3.2 Lagrange polynomial approach for the solution of the piecewise differential equation

In this subsection, the numerical algorithm for the considered equation describing the interactions between prey, predators, and infected prey is presented, using the Lagrange polynomial method outlined in [20]. We begin with a pattern with the case of AB and CF fractional derivative:

$$\begin{aligned} {}_0^{ABC}D_t^\kappa \Pi(t) &= F(\Pi, t), \quad 0 \leq t \leq t_1. \\ {}_{t_1}^{CF}D_t^\kappa \Sigma(t) &= G(\Sigma, t), \quad t_1 \leq t \leq \widehat{T}. \end{aligned} \quad (41)$$

Through the application of the corresponding integral, the following is written

$$\begin{aligned} \eta_m(t) &= \eta_m(0) + (1 - \kappa) \chi_m(t, \eta(t)) + \frac{\kappa}{\Gamma(\kappa)} \int_0^t \chi_m(\vartheta, \eta_m(\vartheta)) (t - \vartheta)^{\kappa-1} d\vartheta, \quad m = 1, 2, \quad 0 \leq t \leq t_1 \\ \eta_n(t) &= \eta_n(t_1) + (1 - \kappa) \chi_n(t_{\nu+1}, \eta^{\nu+1}) + \kappa \int_{t_1}^t \chi_n(\vartheta, \eta(\vartheta)) d\vartheta, \quad n = 1..3, \quad t_1 \leq t \leq \widehat{T} \end{aligned} \quad (42)$$

At $t = t_{\nu+1}$, the above system is converted to:

$$\begin{aligned} \eta_m(t_{\nu+1}) &= \eta_m(0) + (1 - \kappa) \chi_m(t, \eta(t)) + \frac{\kappa}{\Gamma(\kappa)} \int_0^{t_{\nu+1}} \chi_m(\vartheta, \eta_m(\vartheta)) (t_{\nu+1} - \vartheta)^{\kappa-1} d\vartheta, \quad m = 1, 2, \quad 0 \leq t \leq t_1, \\ \eta_n(t_{\nu+1}) &= \eta_n(t_1) + (1 - \kappa) \chi_n(t_{\nu+1}, \eta^{\nu+1}) + \kappa \int_{t_1}^{t_{\nu+1}} \chi_n(\vartheta, \eta(\vartheta)) d\vartheta, \quad n = 1..3, \quad t_1 \leq t \leq \widehat{T} \end{aligned} \quad (43)$$

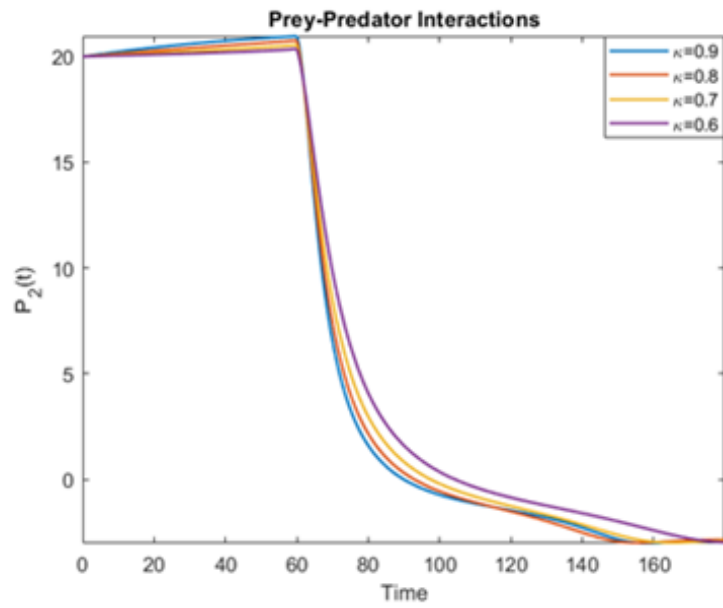
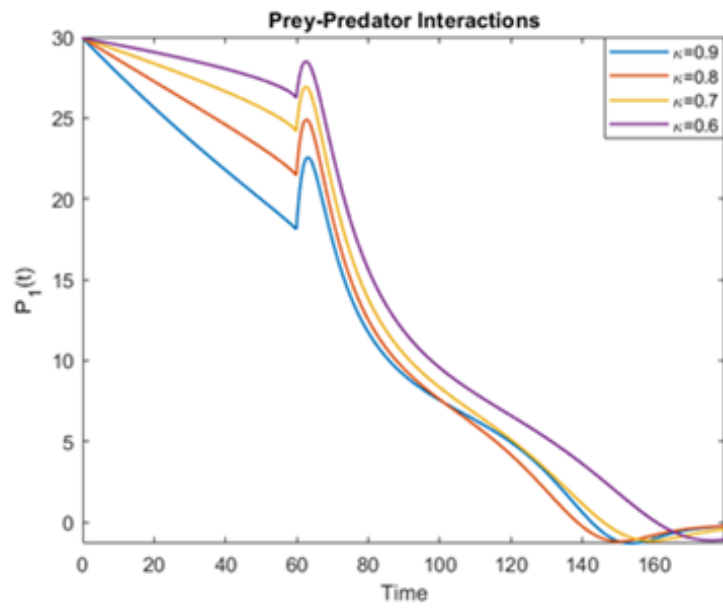
Then, the piecewise model with Atangana-Baleanu and Caputo-Fabrizio derivative is solved numerically by the following scheme [20]:

$$\begin{aligned} \eta_m^{\nu+1} &= \eta_m(0) + (1 - \kappa) \chi_m(t_{\nu+1}, \eta^{\nu+1}) + \frac{\kappa h^\kappa}{\Gamma(\kappa+2)} \sum_{\omega=0}^{\nu_1} \frac{\chi_m(t_{\omega}, \eta_m^\omega)}{h} \left[\begin{array}{l} (\nu_1 - \omega + 1)^\kappa (\nu_1 - \omega + 2 + \kappa) \\ - (\nu_1 - \omega)^\kappa (\nu_1 - \omega + 2 + 2\kappa) \end{array} \right] \\ &\quad - \frac{\kappa h^\kappa}{\Gamma(\kappa+2)} \sum_{\omega=0}^{\nu_1} \frac{\chi_m(t_{\omega-1}, \eta_m^{\omega-1})}{h} \left[\begin{array}{l} (\nu_1 - \omega + 1)^{\kappa+1} \\ - (\nu_1 - \omega)^\kappa (\nu_1 - \omega + 1 + \kappa) \end{array} \right] \\ &\quad m = 1, 2, \quad 0 \leq t \leq t_1. \\ \eta_n^{\nu+1} &= \eta_n(t_1) + (1 - \kappa) \chi_n(t_{\nu+1}, \eta^{\nu+1}) + \frac{\kappa h}{2} \sum_{\omega=\nu_1+1}^{\nu} [3\chi_n(t_\nu, \eta^\nu) - \chi_n(t_{\nu-1}, \eta^{\nu-1})] \\ &\quad n = 1..3, \quad t_1 \leq t \leq \widehat{T}. \end{aligned} \quad (44)$$

The initial conditions and parameters are considered for the case with Atangana-Baleanu and Caputo-Fabrizio derivative (also classical and Caputo derivative) as follows:

$$\begin{aligned} P_1(0) &= 30; I(0) = 0; P_2(0) = 20; a = 0.001; k = 0.001; \theta = 0.05; \sigma = 0.25; \\ a_1 &= 0.101; \rho = 0.7; \mu = 0.265; b = 0.0001; c = 0.0035; \gamma = 0.02. \end{aligned} \quad (45)$$

It is worth noting that a will be taken as a_1 for the second interval of the piecewise differential equation. Figure 3 provides the numerical simulations of the model, incorporating both the Atangana-Baleanu and the fractional derivatives with exponential decay kernel.



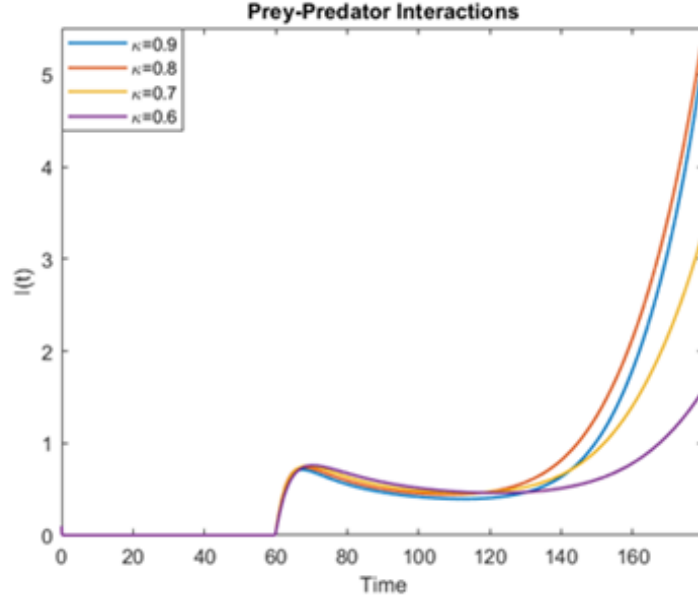


Figure 3. The visual representation for the equation modeling the gradual incorporation of infected prey into ecological system for $\kappa = 0.9$.

We proceed with an another scenario where first interval is with Caputo fractional derivative and second interval is with the classical derivative. Such model is represented by the following:

$$\begin{aligned} {}_0^C D_t^\kappa \Pi(t) &= F(\Pi, t), \quad 0 \leq t \leq t_1. \\ \frac{d}{dt} \Sigma(t) &= G(\Sigma, t), \quad t_1 \leq t \leq \hat{T}. \end{aligned} \quad (46)$$

The corresponding integral [21, 22, 23] is applied to both sides, resulting in

$$\begin{aligned} \eta_m(t) &= \eta_m(0) + \frac{1}{\Gamma(\kappa)} \int_0^t \chi_m(\vartheta, \eta_m(\vartheta)) (t - \vartheta)^{\kappa-1} d\vartheta, \quad m = 1, 2, \quad 0 \leq t \leq t_1 \\ \eta_n(t) &= \eta_n(t_1) + \int_{t_1}^t \chi_n(\vartheta, \eta(\vartheta)) d\vartheta, \quad n = 1..3, \quad t_1 \leq t \leq \hat{T} \end{aligned} \quad (47)$$

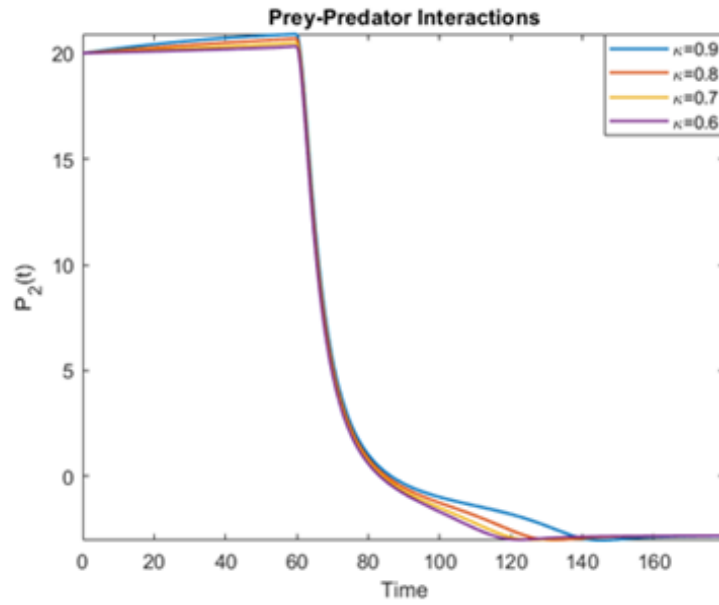
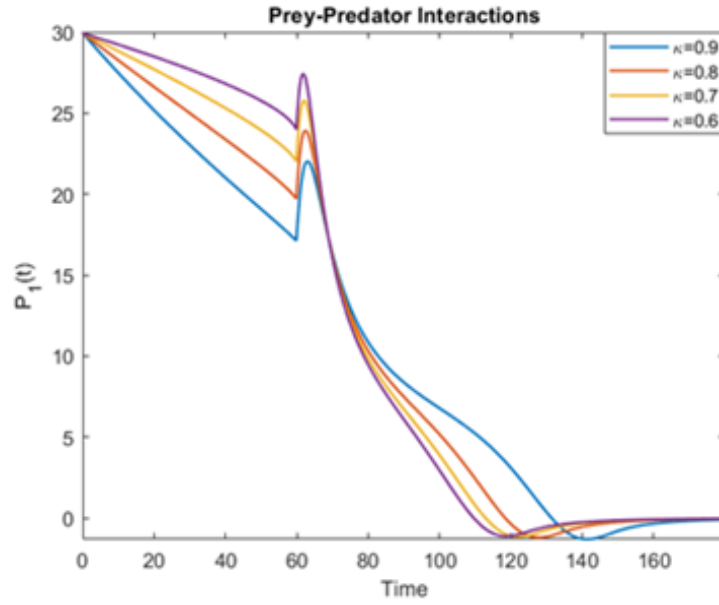
At $t = t_{\nu+1}$, the following equality is written as follows:

$$\begin{aligned} \eta_m(t_{\nu+1}) &= \eta_m(0) + \frac{1}{\Gamma(\kappa)} \int_0^{t_{\nu+1}} \chi_m(\vartheta, \eta_m(\vartheta)) (t_{\nu+1} - \vartheta)^{\kappa-1} d\vartheta, \quad m = 1, 2, \quad 0 \leq t \leq t_1, \\ \eta_n(t_{\nu+1}) &= \eta_n(t_1) + \int_{t_1}^{t_{\nu+1}} \chi_n(\vartheta, \eta(\vartheta)) d\vartheta, \quad n = 1..3, \quad t_1 \leq t \leq \hat{T} \end{aligned} \quad (48)$$

By employing Lagrange polynomial method, the numerical solution of the piecewise differential equation with Atangana-Baleanu and Caputo-Fabrizio derivative is achieved by

$$\begin{aligned} \eta_m^{\nu+1} &= \eta_m(0) + \frac{h^\kappa}{\Gamma(\kappa+2)} \sum_{\omega=0}^{\nu_1} \frac{\chi_m(t_\omega, \eta_m^\omega)}{h} \left[\begin{aligned} &(\nu_1 - \omega + 1)^\kappa (\nu_1 - \omega + 2 + \kappa) \\ &- (\nu_1 - \omega)^\kappa (\nu_1 - \omega + 2 + 2\kappa) \end{aligned} \right] \\ &- \frac{h^\kappa}{\Gamma(\kappa+2)} \sum_{\omega=0}^{\nu_1} \frac{\chi_m(t_{\omega-1}, \eta_m^{\omega-1})}{h} \left[\begin{aligned} &(\nu_1 - \omega + 1)^{\kappa+1} \\ &- (\nu_1 - \omega)^\kappa (\nu_1 - \omega + 1 + \kappa) \end{aligned} \right] \\ & \quad m = 1, 2, \quad 0 \leq t \leq t_1. \\ \eta_n^{\nu+1} &= \eta_n(t_1) + \frac{h}{2} \sum_{\omega=\nu_1+1}^{\nu} [3\chi_n(t_\omega, \eta^\omega) - \chi_n(t_{\omega-1}, \eta^{\omega-1})] \\ & \quad n = 1..3, \quad t_1 \leq t \leq \hat{T}. \end{aligned} \quad (49)$$

Figure 4 illustrates the numerical simulations of the model, integrating the fractional derivative with power-law kernel and classical derivatives.



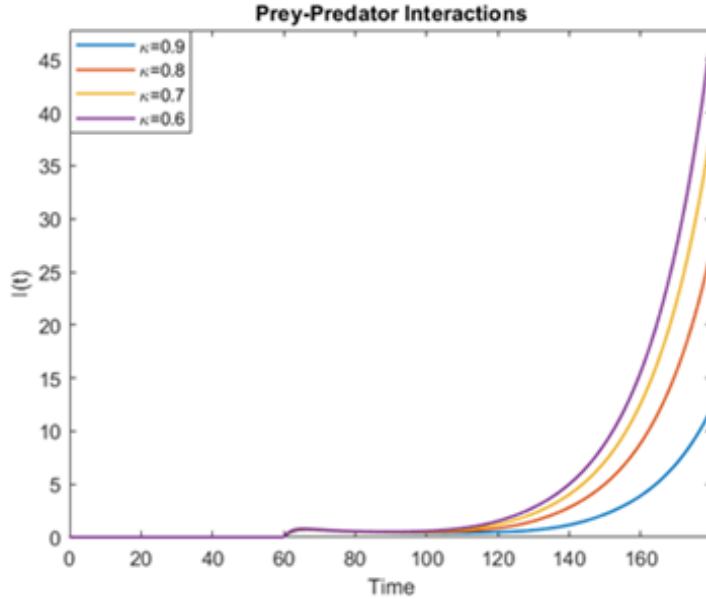


Figure 4. The visual representation for the equation modeling the gradual incorporation of infected prey into ecological system for $\kappa = 0.9$.

4 Gradual incorporation of infected prey into the predator-prey system with consideration of seasonality

In this section, we aim to incorporate seasonality into the considered scenario. Specifically, we will examine the solutions of the modified model, which is derived by using several almost periodic functions in place of the system parameters. This modification aims to effectively capture the seasonal variations inherent in the system. Before presenting such a model, we shall give the definition of almost periodic function. Let us assume the existence of a constant $l(\kappa) > 0$ such that every interval of length $l(\kappa)$ contains at least one value \hat{T} . For each $\kappa > 0$ and $t \in \mathbb{R}$, the function ψ is considered an almost periodic function if it satisfies the following inequality:

$$\left| \psi \left(t + \hat{T} \right) - \psi (t) \right| < \kappa \quad (50)$$

The space of all almost periodic functions on \mathbb{R} , commonly denoted by $AP(\mathbb{R})$, forms a Banach space with the supremum norm. An example of an almost periodic function can be selected as $\sin \left(\frac{2\pi t}{\log 2} \right) + \sin \left(\frac{2\pi t}{\log 5} \right)$.

The model incorporating the aforementioned almost periodic functions can be formulated as follows:

$$\begin{cases} \frac{dP_1}{dt} = aP_1 - bP_1 - \mu(t)P_1P_2, \\ \frac{dP_2}{dt} = \theta(t)P_1P_2 - \rho P_2 \end{cases}, \text{ if } 0 \leq t \leq t_1, \quad (51)$$

$$\begin{cases} \frac{dP_1}{dt} = a(P_1 + I) - bP_1 - cP_1(P_1 + I) - kIP_1 - \mu(t)P_1P_2, \\ \frac{dI}{dt} = kIP_1 - bI - cP_1(P_1 + I) - \gamma(t)IP_2, \\ \frac{dP_2}{dt} = \theta(t)P_1P_2 - \sigma IP_2 - \rho P_2 \end{cases}, \text{ if } t_1 \leq t \leq \widehat{T},$$

where

$$\begin{aligned} \mu(t) &= a_1 \cos(\pi t) + b_1 \cos(\vartheta(t)), \\ \theta(t) &= a_2 \cos(\pi t) + b_2 \cos(\vartheta(t)), \\ \gamma(t) &= a_3 \cos(\pi t) + b_3 \cos(\vartheta(t)). \end{aligned} \quad (52)$$

We next consider the following piecewise differential equation

$$\begin{aligned} \frac{d}{dt}\Pi(t) &= F(\Pi, t), \quad 0 \leq t \leq t_1. \\ {}^C D_t^\kappa \Sigma(t) &= G(\Sigma, t), \quad t_1 \leq t \leq \widehat{T}. \end{aligned} \quad (53)$$

The corresponding integral is applied to both sides, resulting in

$$\begin{aligned} \eta_m(t) &= \eta_m(0) + \int_0^t \chi_m(\vartheta, \eta_m(\vartheta)) d\vartheta, \quad m = 1, 2, 0 \leq t \leq t_1 \\ \eta_n(t) &= \eta_n(t_1) + \frac{1}{\Gamma(\kappa)} \int_{t_1}^t \chi_n(\vartheta, \eta(\vartheta)) (t - \vartheta)^{\kappa-1} d\vartheta, \quad n = 1..3, t_1 \leq t \leq \widehat{T} \end{aligned} \quad (54)$$

At $t = t_{\nu+1}$, we obtain the following:

$$\begin{aligned} \eta_m(t_{\nu+1}) &= \eta_m(0) + \int_0^{t_{\nu+1}} \chi_m(\vartheta, \eta_m(\vartheta)) d\vartheta, \quad m = 1, 2, 0 \leq t \leq t_1, \\ \eta_n(t_{\nu+1}) &= \eta_n(t_1) + \frac{1}{\Gamma(\kappa)} \int_{t_1}^{t_{\nu+1}} \chi_n(\vartheta, \eta(\vartheta)) (t_{\nu+1} - \vartheta)^{\kappa-1} d\vartheta, \quad n = 1..3, t_1 \leq t \leq \widehat{T} \end{aligned} \quad (55)$$

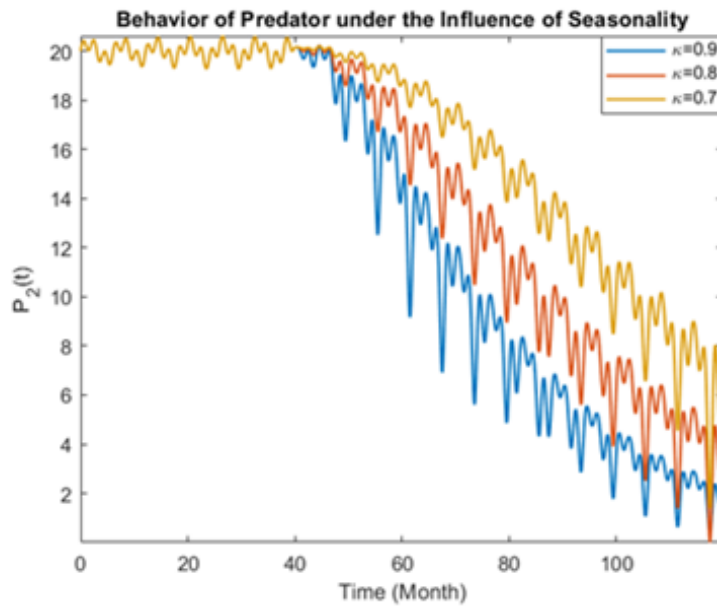
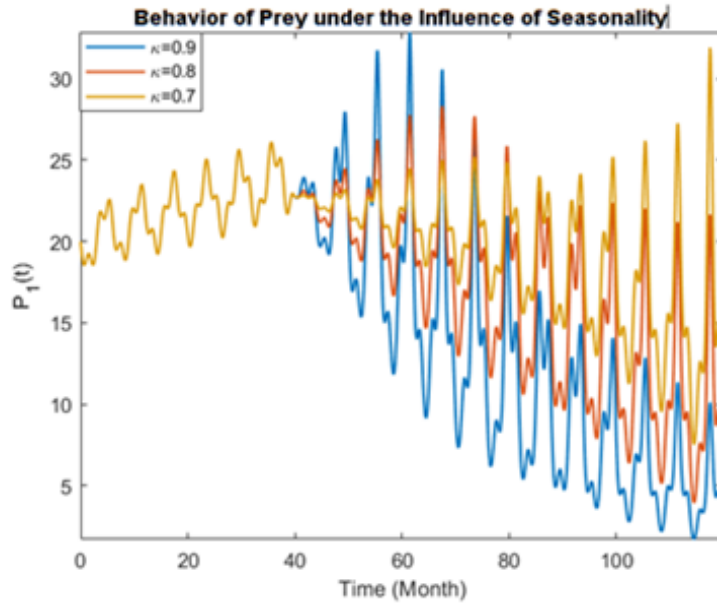
Then, the numerical scheme based on Lagrange polynomial approach for piecewise system is represented by the following:

$$\begin{aligned} \eta_m^{\nu+1} &= \eta_m(0) + \frac{h}{2} \sum_{\omega=0}^{\nu_1} [3\chi_n(t_\nu, \eta^\nu) - \chi_n(t_{\nu-1}, \eta^{\nu-1})] \\ & \quad m = 1, 2, 0 \leq t \leq t_1. \\ \eta_n^{\nu+1} &= \eta_n(t_1) + \frac{h^\kappa}{\Gamma(\kappa+2)} \sum_{\omega=\nu_1+1}^{\nu} \frac{\chi_m(t_\omega, \eta_m^\omega)}{h} \begin{bmatrix} (\nu_1 - \omega + 1)^\kappa (\nu_1 - \omega + 2 + \kappa) \\ -(\nu_1 - \omega)^\kappa (\nu_1 - \omega + 2 + 2\kappa) \end{bmatrix} \\ & \quad - \frac{h^\kappa}{\Gamma(\kappa+2)} \sum_{\omega=\nu_1+1}^{\nu} \frac{\chi_m(t_{\omega-1}, \eta_m^{\omega-1})}{h} \begin{bmatrix} (\nu_1 - \omega + 1)^{\kappa+1} \\ -(\nu_1 - \omega)^\kappa (\nu_1 - \omega + 1 + \kappa) \end{bmatrix} \\ & \quad n = 1..3, t_1 \leq t \leq \widehat{T}. \end{aligned} \quad (56)$$

The initial conditions and parameters are considered for the case with classical and Caputo derivative as follows:

$$\begin{aligned} P_1(0) &= 20; I(0) = 0; P_2(0) = 20; a = 0.005; k = 0.001; \theta = 0.15; \\ \sigma &= 0.07; \rho = 0.007; \mu = 0.265; b = 0.004; c = 0.0035; \\ a_1 &= 4; b_1 = 3; a_2 = 3; b_2 = 1; a_3 = 1; b_3 = 3; \gamma = 0.02. \end{aligned} \quad (57)$$

In Figure 5, we perform the numerical visualization of the modified model, incorporating integer and noninteger orders, providing a seasonal visualization of the system's behavior under these fractional-order operators.



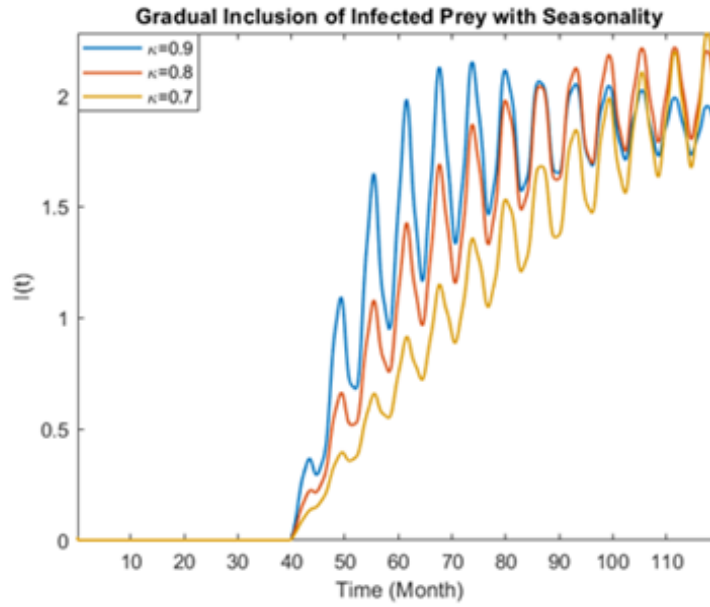
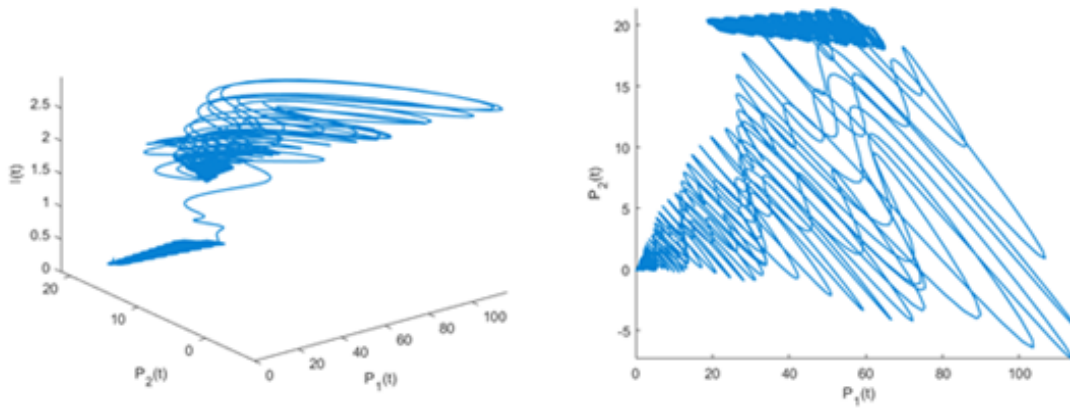


Figure 5. The visual representation for the equation modeling the gradual incorporation of infected prey into ecological system for different fractional orders.

The 3D visualization of dynamics of the considered equation with classical and Caputo derivative is shown in Figure 6.



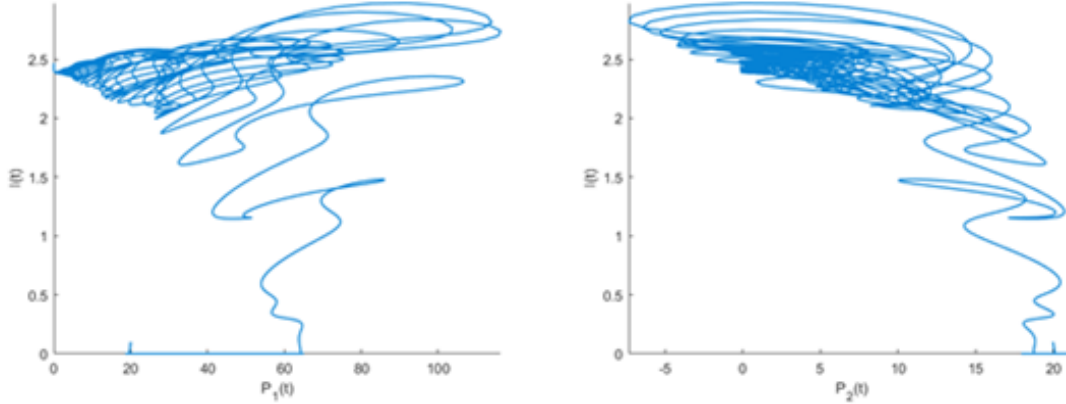


Figure 6. The visual representation for the equation modeling the gradual incorporation of infected prey into ecological system for $\kappa = 0.9$.

5 Conclusion

This study focused on modeling the introduction of infected prey into a population containing prey and predator over time. We know that infected prey may exhibit changes in behavior or reduced fitness, making them more susceptible to predation and affecting interactions between prey and predator populations. To provide a more accurate representation of these dynamics, disease transmission and its effects on species behavior, survival, and ecosystem stability were included in the model. The gradual introduction of infected prey was modeled using an advanced piecewise differential equation approach that integrated fractional derivatives to account for memory effects and non-local behaviors. Additionally, nearly periodic functions were included to incorporate seasonality, effectively capturing the cyclical nature of environmental fluctuations. This comprehensive framework provides a more realistic and dynamic understanding of predator-prey interactions, especially in the presence of disease.

References

- [1] Hethcote H.W., Wang W.D., Han L., Ma Z.E., A predator–prey model with infected prey, *Theor Popul Biol*, 66 (2004), pp. 259-268.
- [2] Yamada Y. Stability of steady-states for prey-predator diffusion equations with homogeneous Dirichlet conditions. *SIAM J Math Anal* 1990;21:327–45.
- [3] Iğret Araz S., Boubekeur MA., Piecewise differential equations for prey-predator interactions: From dyadic to triadic, *Iranian Journal of Science* 48, 1613–1624.
- [4] Li S., Wang X., Analysis of a stochastic predator–prey model with disease in the predator and Beddington–DeAngelis functional response, *Adv. Difference Equ.*, 224 (2015).
- [5] Dutta H., *Mathematical Modelling in Health, Social and Applied Sciences*, Springer, 2020.
- [6] Elettrey, M.F.: Two-prey one-predator model. *Chaos Solitons Fractals* 39(5), 2018–2027 (2009).

- [7] Gao Y., Banerjee M., Ta TV., Dynamics of infectious diseases in predator–prey populations: A stochastic model, sustainability, and invariant measure, *Mathematics and Computers in Simulation*, 227, 2025, 103-120.
- [8] Djilali, S., Ghanbari, B. Dynamical behavior of two predators–one prey model with generalized functional response and time-fractional derivative. *Adv Differ Equ* 2021, 235 (2021).
- [9] Yang Y., Meng F., Xu Y., Global bifurcation analysis in a predator–prey system with simplified Holling IV functional response and antipredator behavior, *Mathematical Methods in the Applied Sciences*, 46 (5), 2023.
- [10] Shang Z., Qiao Y., Bifurcation analysis in a predator–prey model with strong Allee effect on prey and density-dependent mortality of predator, *Mathematical Methods in the Applied Sciences*, 47 (4), 2024.
- [11] Wang M., Yao S., The dynamics of an eco-epidemiological prey–predator model with infectious diseases in prey, *Communications in Nonlinear Science and Numerical Simulation*, 132, 2024.
- [12] Iğret Araz S., Seasonality of Ricker mutualism model employing rate indicator with almost periodic function, hal-04786606, 2024.
- [13] Atangana A., Iğret Araz S., Piecewise differential equations: Theory, methods and applications, *AIMS Mathematics*, 8, (7), 2023.
- [14] Shah K., Abdeljawad T., Alrabaiah H., On coupled system of drug therapy via piecewise equations, *Fractals*, Vol. 30, No. 8 (2022).
- [15] Caputo M., Linear model of dissipation whose Q is almost frequency independent. II. *Geophysical Journal International*. 13 (5): 1967, 529-539.
- [16] Caputo M., Fabrizio M., On the notion of fractional derivative and applications to the hysteresis phenomena. *Mechanica* 52(13), 2017, 3043-3052.
- [17] Atangana A., Baleanu D., New fractional derivatives with non-local and non-singular kernel, Theory and Application to Heat Transfer Model, *Thermal Science*, 20 (2), 2016, 763-769.
- [18] Podlubny I., *Fractional differential equations*, vol. 198 of *Mathematics in Science and Engineering*, Academic Press, San Diego, 1999, ISBN: 9780125588409.
- [19] Atangana A., Iğret Araz S., Step forward on nonlinear differential equations with the Atangana-Baleanu derivative: Inequalities, existence, uniqueness and method, *Chaos, Solitons& Fractals*, 173.
- [20] Mekkaoui T., Atangana A., New numerical approximation of fractional derivative with non-local and non-singular kernel: Application to chaotic model, 2017, 132, (2017).
- [21] Atangana A., Iğret Araz S., New concept in calculus: Piecewise differential and integral operators, *Chaos, Solitons Fractals*, 145 (2021).
- [22] Akbulut Arık I., Iğret Araz S., Crossover behaviors via piecewise concept: A model of tumor growth and its response to radiotherapy, *Results in Physics*, 41, 2022.
- [23] Iğret Araz S., Çetin MA., Fractal-Fractional Modeling of the Covid-19 Spread with Deterministic and Stochastic Approaches, *International Journal of Applied and Computational Mathematics* 11 (1), 1-30, 2025.